FERMILAB-CONF-08-280-E

Hadron Collider Physics Symposium (HCP2008), Galena, Illinois, USA

Mixing and CP Violation at the Tevatron

G. Brooijmans, on behalf of the CDF and D0 Experiments
Columbia University, New York, NY, USA

Measurements of meson mixing and CP violation parameters obtained by the CDF and D0 experiments at the Fermilab Tevatron are presented. These include results on B_s and D meson mixing, and searches for CP violation in the decay $B^+ \to J/\psi K^+$, in mixing through semileptonic B_s meson decays, and in the interference between mixing and decay in the process $B_s \to J/\psi\phi$.

1. INTRODUCTION

The Tevatron is a heavy flavor factory in which charm and beauty hadrons of all types are produced at high rates. Even though the hadron collider environment increases the complexity of events, both the CDF and D0 experiments are making critical measurements of meson mixing and CP violation parameters. CDF exploits its large level one trigger bandwidth and level two impact parameter trigger to collect large samples of long-lived particles, and uses dE/dx and time-of-flight measurements to suppress backgrounds. D0 benefits from its large acceptance for muons to collect large semileptonic samples. In this paper, a number of unique results are presented: the measurements of B_s and D meson mixing parameters, and searches for CP violation in the decay $B^+ \to J/\psi K^+$, in mixing through semileptonic B_s meson decays, and in the interference between mixing and decay in the process $B_s \to J/\psi\phi$. Throughout this paper, charge conjugated modes are implicitly assumed.

2. MESON MIXING

Because the neutral meson mass eigenstates can be a linear combination of the weak eigenstates, they can mix. Taking for example B mesons, we can write[1]

$$|B_{L,H}\rangle = p|B_f^0\rangle + q|\bar{B}_f^0\rangle, \tag{1}$$

where $B_{H,L}$ are the mass eigenstates and $B_f^0, \bar{B}_f^0$ are the weak (or flavor) eigenstates. The mass eigenstates then have masses $m_{H,L} = M \pm \frac{\Delta m}{2}$ and lifetimes $\Gamma_{H,L} = \Gamma \pm \frac{\Delta\Gamma}{2}$. Because of the mass difference, a state produced as $B^0(\bar{B}^0)$ can oscillate between B^0 and $\bar{B}^0$ and decay as $\bar{B}^0(B^0)$, with a characteristic oscillation frequency Δm. In addition to the variables Δm and $\Delta\Gamma$, it is usual to define

$$x = \frac{\Delta m}{\Gamma},\ y = \frac{\Delta\Gamma}{2\Gamma} \tag{2}$$

and

$$x' = x\cos\delta + y\sin\delta, y' = -x\sin\delta + y\cos\delta, \tag{3}$$

which are useful when treating integral oscillation probabilities. Here δ is a strong phase.

2.1. B_s Meson Mixing

From the point of view of Feynman diagrams, B meson mixing is dominated by box diagrams with W bosons and up-type quarks in the internal lines. Since V_{tb} is large, diagrams with top quarks are dominant and the oscillation

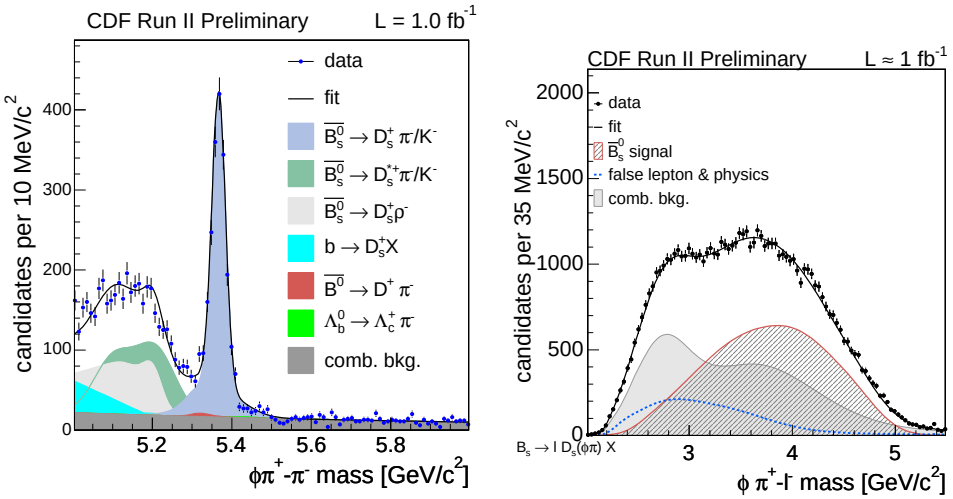

(a) (b)

Figure 1: Reconstructed B_s candidate mass in a hadronic (left) and semi-leptonic (right) channel at CDF.

frequency is proportional to m^2_{top}/m^2_W. The high oscillation frequency of B mesons was in fact the first experimental indication of a very large top quark mass [2, 3], and this process is in general sensitive to loop-level contributions from new heavy particles. Since $V_{ts} > V_{td}$, B_s meson oscillations are faster than B_d oscillations and the frequency is correspondingly more difficult to measure.

The analysis strategy for the measurement of the B_s meson mixing frequency, and most of the other measurements described here, consists in two main parts. On the "reconstructed side", we have the B_s meson under study: its flavor at decay time is given by the charges of the decay products, and it is then sufficient to measure its momentum and transverse decay length to determine its proper lifetime. To tag the quark flavor at production time, either the "opposite side" b-hadron is used, exploiting the fact that at the Tevatron the vast majority of b quarks are produced in pairs, or the "same side" hadron from fragmentation is identified. In the case of B_s meson production, this is likely to be a K meson.

The B_s meson reconstruction proceeds through the reconstruction of the decay chain $B_s \to D_s X$, where X can be leptons, or one or three pions. Multiple D_s decay channels are considered. While the semi-leptonic channels allow for a higher trigger efficiency, they suffer from higher backgrounds and a significantly worse B_s meson momentum determination due to the escaping neutrino. This is seen in Fig. 1 where the reconstructed B_s candidate mass is shown for a hadronic and semi-leptonic channel used in CDF.

The flavor of the B_s meson at production is determined using opposite-side tagging variables that include lepton charge, jet charge and secondary vertex charge, and same-side tagging based on the charge of a nearby hadron. Both experiments use multivariate techniques to combine the various opposite- and same-side tagging variables: CDF uses a neural network and D0 uses a likelihood. To verify the performance (efficiency and dilution) of the flavor tagging algorithm, the B_d oscillation frequency is measured [4, 5] and compared to the world average.

To measure the oscillation frequency, it is necessary to extract all the information on an event-by-event basis, giving events weights in the extraction of the result that are proportional to their probability of originating from a certain source. In both experiments, an unbinned maximum likelihood fit is used. Figure 2 shows the measured B_s meson oscillation frequency in the form of a scan over the likelihood function output. CDF has significantly better sensitivity thanks to much larger level one trigger bandwidth, a secondary vertex trigger at level two, and particle identification based on dE/dx in the tracker and a time-of-flight detector. This allows CDF to exploit the excellent resolution of the hadronic channels; they measure [6] $\Delta m_s = 17.77 \pm 0.10(stat) \pm 0.07(syst) ps^{-1}$ with a signal larger than 5σ. In D0, where the signal is dominated by the semileptonic channels, the signal has a significance of 3σ and the measured value is [7, 8] $\Delta m_s = 18.53 \pm 0.93(stat) \pm 0.30(syst) ps^{-1}$.

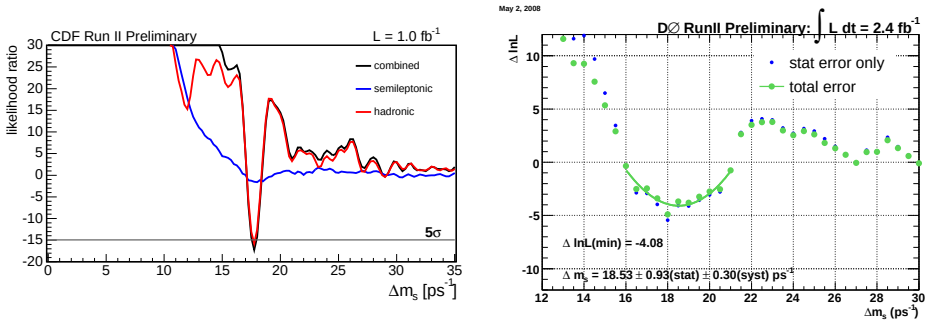

(a) (b)

Figure 2: Measurement of the B_s meson mixing frequency. The result is shown in the form of a scan over the value of the likelihood function for CDF (left) and D0 (right).

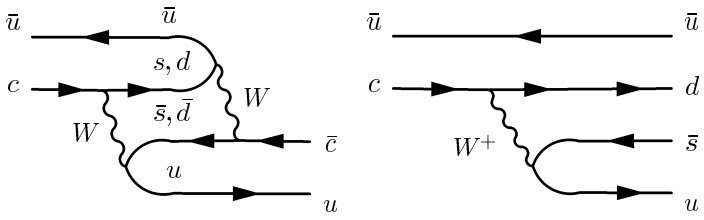

(a) (b)

Figure 3: Left: dominant "long range" contribution to D meson mixing. The process goes through an intermediate virtual π or K meson. Right: doubly cabibbo-suppressed decay.

2.2. D Meson Mixing

As opposed to B meson oscillations, D mesons are expected to oscillate very slowly in the standard model. This is because the box diagram, with $\Delta C = 2$, is very small due to a combination of CKM and GIM suppressions. The dominant contribution comes from the "long range" $(2 \times \Delta C = 1)$ diagram shown in Fig. 3, and is too small to make the oscillation observable before decay. The effect of mixing can however possibly be seen through its interference in the doubly Cabibbo-suppressed $D^0 \to K^+\pi^-$ decay (right panel of Fig. 3).

The analysis [9] looks for a mixing-induced time dependence of the ratio of $(D^0 \to K^+\pi^-)/(D^0 \to K^-\pi^+)$ decays in a sample of events collected using CDF's impact parameter trigger. In this case, the flavor of the D^0 meson at production is tagged by selecting the decay $D^{*+} \to \pi^+ D^0, D^0 \to K\pi$ chain. To reduce backgrounds, particle identification (PID) is applied as in the B_s mixing analysis, and $K\pi$ candidates that fall into the D^0 mass window with both mass assignments to the reconstructed tracks are rejected (PID separation has limited discriminating power). Events are then selected using the $\Delta m = m(K\pi\pi) - m(K\pi) - m(\pi)$ distributions shown in Fig. 4.

Figure 5 shows the results of the analysis. On the left, the ratio of doubly Cabibbo-suppressed over Cabibbo-favored decays as a function of proper decay time exhibits the parabolic dependence

$$R(t) = R_D + \sqrt{R_D} y' t + \frac{x'^2 + y'^2}{4} t^2 \tag{4}$$

expected in the presence of mixing, where x', y' are the mixing parameters defined in section 2. The χ^2/dof for the parabolic (flat) fit is 19.2/17 (36.8/19) The right plot shows the probability intervals in the (x'^2, y') plane. The best fit is 3.8σ away from the null hypothesis.

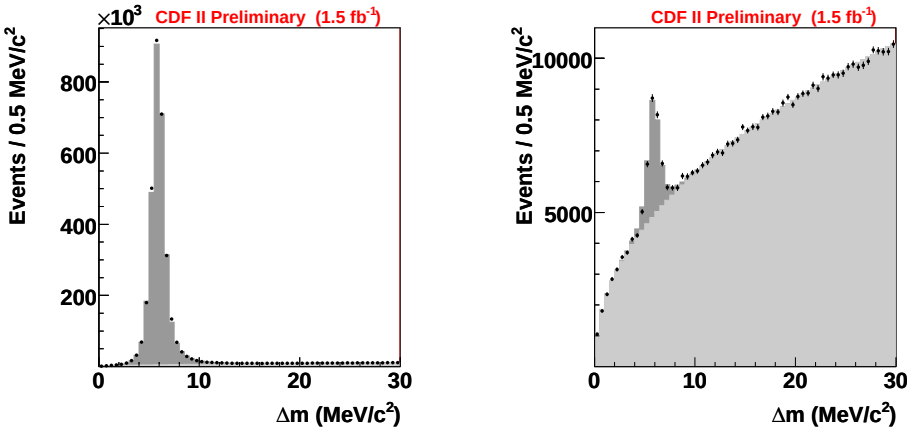

(a) (b)

Figure 4: $\Delta m = m(K\pi\pi) - m(K\pi) - m(\pi)$ distributions for Cabibbo-favored (left) and doubly Cabibbo-suppressed candidates (right). The combinatorial background and signal are shown in light and dark grey respectively.

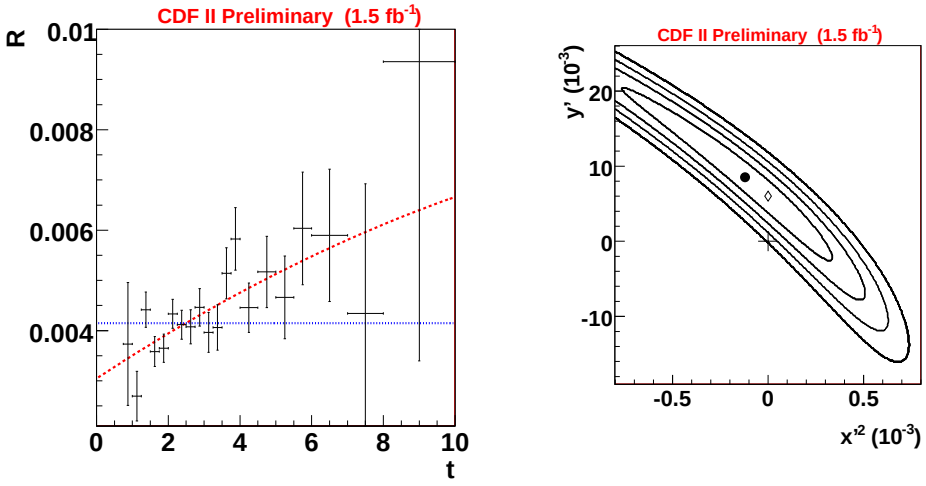

(a) (b)

Figure 5: Ratio of doubly Cabibbo-suppressed over Cabibbo-favored decays as a function of proper decay time (left), and (bayesian) probability intervals for the mixing parameters (x'^2, y') (right).

3. CP VIOLATION

In this paper, CP violation measurements are split in three categories:

- CP violation in the decay amplitudes, where $\Gamma(B \to f) \neq \Gamma(CP(B) \to CP(f))$. In charged meson decays, this is the only possible manifestation of CP violation, and a measurement in the $B^+ \to J/\psi K^+$ channel is described.
- CP violation in mixing, which can be detected through an asymmetry in charged-current neutral meson decays. Recent results from inclusive same-sign dimuon events and exclusive $B_s \to \mu^+ \nu D_s^- X$ decays are given.
- CP violation in the interference between mixing and decay can be tested in decays with and without mixing to a single final state. Here, studies in the $B_s \to J/\psi\phi$ channel are presented.

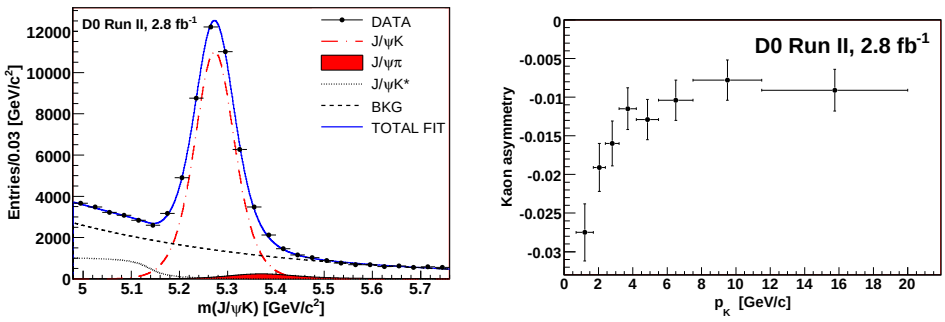

(a) (b)

Figure 6: Left: B^+ candidate mass distribution showing the data and contributions extracted from a fit to the data. The shapes of the various contributions are extracted from the simulation. Right: kaon reconstruction asymmetry as a function of kaon momentum.

3.1. CP Violation in Decays

D0 selects a $B^+ \to J/\psi K^+(\pi^+)$ sample [10] where the J/ψ decays to a pair of muons. This yields a very clean sample with approximately 40,000 candidates as shown in the left panel of Fig. 6. To determine the asymmetry, the sample is divided in 8 subsamples based on solenoid polarity β, sign γ of the $J/\psi K^+$ system pseudo-rapidity η, and kaon charge q:

$$n_q^{\beta\gamma} = \frac{1}{4} N \epsilon^\beta (1 + qA)(1 + q\gamma A_{fb})(1 + \gamma A_{det})(1 + q\beta\gamma A_{ro})(1 + q\beta A_{q\beta})(1 + \beta\gamma A_{\beta\gamma}), \tag{5}$$

where N is the total number of events in the sample, ϵ^β is the fraction of integrated luminosity taken with solenoid polarity β, A is the CP-violating asymmetry, A_{fb} is the forward-backward asymmetry and all other asymmetries are potentially generated by the detector. The total number of events in the $J/\psi K^+$ and $J/\psi\pi^+$ channels, the fraction of integrated luminosity for each solenoid polarity and the asymmetries are determined from a fit using the number of events in each subsample for inputs. The forward-backward symmetry, as well as all detector asymmetries are found to be compatible with zero. At this stage, the observed CP asymmetry needs to be corrected for the asymmetry in kaon reconstruction efficiency induced by the different interactions of K^+ and K^- with the detector, which is made of matter only. This reconstruction efficiency asymmetry is measured from a sample of $D^{*+} \to D^0\pi^+, D^0 \to \mu\nu K^-$ events as a function of kaon momentum (right panel of Fig. 6), and applied to the kaon spectrum in the B^+ sample. After this correction, the CP asymmetries are measured to be $A_{CP}(B^+ \to J/\psi K^+) = 0.0075 \pm 0.0061(stat) \pm 0.0027(syst)$ and $A_{CP}(B^+ \to J/\psi\pi^+) = -0.09 \pm 0.08(stat) \pm 0.03(syst)$. The dominant systematic uncertainty comes from the mass distribution model.

3.2. CP Violation in Mixing

CP violation due to mixing between neutral B mesons can be searched for by measuring the asymmetry in same-sign dimuon events:

$$A_{SL}^{\mu\mu} = \frac{N(b\bar{b} \to \mu^+\mu^+X) - N(b\bar{b} \to \mu^-\mu^-X)}{N(b\bar{b} \to \mu^+\mu^+X) + N(b\bar{b} \to \mu^-\mu^-X)}. \tag{6}$$

Two approaches are used:

- CDF [11] uses all dimuon events but exploits the two-dimensional $(\mu - \mu)$ impact parameter significance distributions to unfold contributions from different sources, including beauty and charm hadrons. CDF finds $A_{SL}^{\mu\mu} = -0.0080 \pm 0.0090(stat) \pm 0.0068(syst)$.

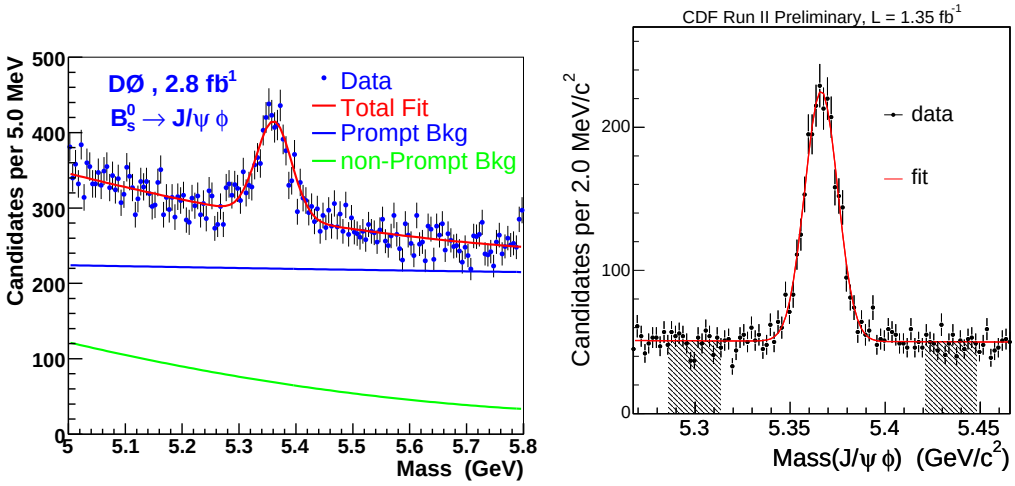

(a) (b)

Figure 7: $B_s \to J/\psi\phi$ candidate samples after event selection in D0 (left) and CDF (right).

- D0 [12] uses all dimuon events, and estimates the contributions from all possible processes to the sample, including sequential decays, Drell-Yan, instrumentals, etc. The "8 subsamples" technique described in section 3.1 is used to extract the asymmetry. D0 measures $A_{SL}^{\mu\mu} = -0.0053 \pm 0.0025(stat) \pm 0.0018(syst)$.

In both cases, the asymmetry from fake muons due to kaons and pions which have asymmetric reconstruction efficiencies (see section 3.1) is determined from data and corrected for.

The flavor-specific asymmetry A_{SL}^s then needs to be derived using the sample composition and the known oscillation probabilities, since $A_{SL}^{\mu\mu}$ has contributions from both B_d and B_s mixing. This is done by taking A_{SL}^d from the B-factories, and the known B_d and B_s production ratios and mixing parameters. The results are:

- CDF: $A_{SL}^s = 0.020 \pm 0.021(stat) \pm 0.016(syst) \pm 0.009(inputs)$;
- D0: $A_{SL}^s = -0.0064 \pm 0.0101(all\ uncertainties\ combined)$.

An alternative approach is to use flavor-specific decays, as is done in the D0 analysis [13] of $B_s \to \mu^+\nu D_s^- X$, where again the asymmetry is determined using the 8 subsamples technique. This yields $A_{SL}^s = 0.0245 \pm 0.0193(stat) \pm 0.0035(syst)$.

3.3. CP Violation in the Interference Between Mixing and Decay

The search for CP violation in the interference of mixing and decay can be searched for in final states that are common to both B_s and $\bar{B}_s$ decays. Both CDF [14] and D0 [15] make flavor-tagged measurements of the CP properties of the $B_s(\bar{B}_s) \to J/\psi\phi$ process. This is similar to the measurement of $\sin(2\beta)$ in $B_d(\bar{B}_d) \to J/\psi K_s$ decays at the B-factories. The angle $\phi_s(= -2\beta_s)$ is however much smaller. An easy way to see this is that the opposing side in the corresponding unitarity triangle is proportional to $\left|\frac{V_{us}V_{ub}^*}{V_{cs}V_{cb}^*}\right|$, whereas for β it is proportional to $\left|\frac{V_{ud}V_{ub}^*}{V_{cd}V_{cb}^*}\right|$. This measurement requires the determination of the CP eigenvalue of the vector-vector $J/\psi\phi$ final state, and benefits from the identification of the flavor of the decaying B_s meson.

Both experiments use events where the J/ψ meson decays to a pair of muons, leading to a high trigger and reconstruction efficiency. At the event selection level, CDF uses a neural network with variables that include PID from dE/dx in the drift chamber and information from the time-of-flight detector. D0 uses a "square cuts" event selection without PID. The resulting B_s meson candidate samples are shown in Fig. 7.

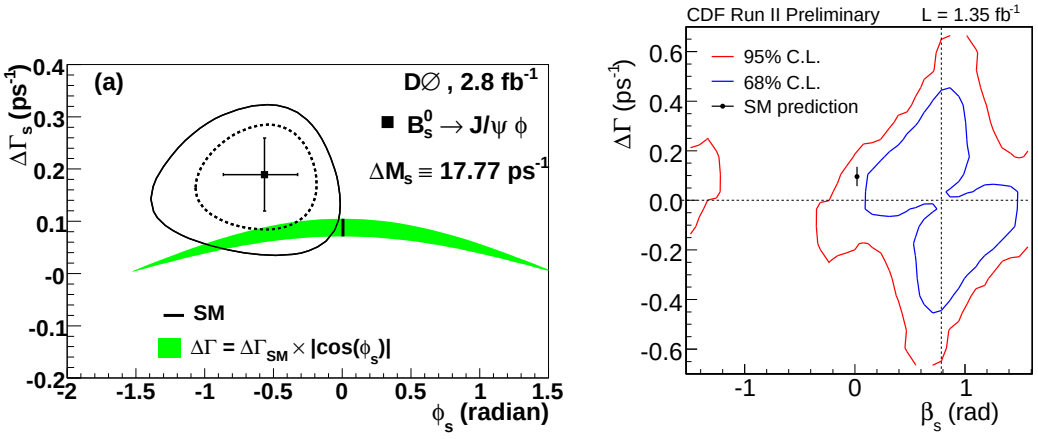

(a) (b)

Figure 8: Two-dimensional confidence intervals in the (β_s,$\Delta\Gamma_s$) plane from the flavor-tagged analysis of $B_s \to J/\psi\phi$ decays from D0 (left) and CDF (right).

Since the $J/\psi\phi$ final state consists of two vector mesons, both CP eigenvalues are possible. The value for a given B_s candidate is measured by determining the relative polarization of the J/ψ and ϕ mesons: the angular dependence of the relative directions of the decay products $\mu^+\mu^-$ and K^+K^- is expressed in the J/ψ restframe ("transversity basis") in terms of this polarization. The corresponding probability density functions are determined from simulation, and used to determine each candidate's probability to be in a given eigenstate. Note that the detector efficiencies are not flat as a function of transversity angles, and this is properly accounted for.

Constraining the flavor of the decaying B_s meson removes a twofold ambiguity in the result. This is achieved by determining the B_s meson flavor at production and using the mixing frequency measured by CDF (see section 2.1). Both experiments use both opposite-side and same-side tags as described in section 2.1. The tagging power obtained in CDF is $\epsilon\mathcal{D}^2 = 1.28\%$ and 3.65% for opposite- and same-side tags respectively, and 4.68% for the combined tag in D0.

To maximize sensitivity, an unbinned likelihood fit is used which assigns event-by-event signal and background probabilities based on reconstruction uncertainties, dilution, accuracy of CP eigenstate determination etc. D0 uses constraints on strong phases from world-average values [16] of measurements of $B_d \to J/\psi K^*$ decays, whereas CDF lets these phases float. Constraining the phases essentially eliminates the remaining ambiguity in the extraction of the result, but there may be differences between the phases in $B_d \to J/\psi K^*$ and $B_s \to J/\psi\phi$ decays. From the likelihood fit, the average lifetime, $\Delta\Gamma_s$, $\phi_s(= -2\beta_s)$, the magnitudes of the polarization amplitudes and the strong phases are extracted.

A small added complication to the extraction of the final CDF result is due to the fact that in that analysis the likelihood profiles are not parabolic close to the minima. Since standard frequentist techniques can't be applied, CDF uses a Feldman-Cousins-like likelihood ratio ordering to build the two-dimensional confidence region in the (β_s,$\Delta\Gamma_s$) plane. The results obtained by CDF and D0 are shown in Fig. 8.

Both experiments measure values that are in reasonable agreement with the standard model: the "standard model probability" is 15% and 7% for the CDF and D0 results respectively. However, it is clear from Fig. 8 that both results pull in the same direction ($\phi_s(= -2\beta_s)$) and with similar magnitudes. While an official combination of these results by the experiments is not ready yet, the UT*fit* collaboration has performed a combined fit of these results [17] with the CP asymmetries described in section 3.2. They try multiple methods to unfold the strong phases constraint from the D0 result, and in each of the methods they find a value of ϕ_s that is 3σ or more away from the standard model prediction. It should be noted that for both CDF and D0, the measurement uncertainties are completely dominated by statistics, so that the results will still improve by quite a bit, hopefully leading to a conclusive statement. If the UT*fit* conclusion

is confirmed (and strengthened), this would be the first evidence for CP violation outside the CKM mechanism.

4. CONCLUSIONS

The beauty and charm physics programs at CDF and D0 continue to produce a large number of excellent results. A number of recent highlights were presented here. CDF has now seen evidence for D meson mixing, and both CDF and D0 are making precise measurements of CP violation asymmetries in B meson mixing and decay. The B_s meson mixing parameters are being pinned down: CDF measures Δm_s with high precision, both experiments find a value of $\Delta\Gamma_s$ in good agreement with the standard model, and both experiments see similar deviations of ϕ_s from the standard model expectation. The latter measurement will become significantly more precise with increasing statistics. If the result is confirmed, this will be the first sign of CP violation in the quark sector outside the CKM mechanism.

Acknowledgments

We thank the staffs at Fermilab and collaborating institutions, and acknowledge support from the DOE and NSF (USA); the A.P. Sloan Foundation (USA); the INFN (Italy); the Ministry of Education, Culture, Sports, Science and Technology (Japan); the Swiss National Science Foundation (Switzerland); the CICT (Spain); the European Community's Human Potential Programme under contract HPRN-CT-2002-00292; the Academy of Finland (Finland); CEA and CNRS/IN2P3 (France); FASI, Rosatom and RFBR (Russia); CNPq, FAPERJ, FAPESP and FUNDUNESP (Brazil); DAE and DST (India); Colciencias (Colombia); CONACyT (Mexico); KRF and KOSEF (Korea); CONICET and UBACyT (Argentina); FOM (The Netherlands); STFC (United Kingdom); MSMT and GACR (Czech Republic); CRC Program, CFI, NSERC and WestGrid Project (Canada); BMBF and DFG (Germany); SFI (Ireland); The Swedish Research Council (Sweden); CAS and CNSF (China); and the Alexander von Humboldt Foundation (Germany).

References

[1] **Particle Data Group** Collaboration, W. M. Yao *et al.*, *J. Phys.* **G33** (2006) 1–1232.
[2] **UA1** Collaboration, C. Albajar *et al.*, *Phys. Lett.* **B186** (1987) 247.
[3] **ARGUS** Collaboration, H. Albrecht *et al.*, *Phys. Lett.* **B192** (1987) 245.
[4] **CDF** Collaboration, T. Aaltonen *et al.*, "Measurement of B0 Oscillations and Calibration of Flavor Tagging in Semileptonic Decays." CDF Note 8235, 2006.
[5] **D0** Collaboration, V. M. Abazov *et al.*, *Phys. Rev.* **D74** (2006) 112002, arXiv:hep-ex/0609034.
[6] **CDF** Collaboration, A. Abulencia *et al.*, *Phys. Rev. Lett.* **97** (2006) 242003, arXiv:hep-ex/0609040.
[7] **D0** Collaboration, V. M. Abazov *et al.*, *Phys. Rev. Lett.* **97** (2006) 021802, arXiv:hep-ex/0603029.
[8] **D0** Collaboration, V. M. Abazov *et al.*, "(Combined) Measurement of the Flavor Oscillation Frequency of B_s Mesons." D0 note 5474, 2007.
[9] **CDF** Collaboration, T. Aaltonen *et al.*, *Phys. Rev. Lett.* **100** (2008) 121802, arXiv:0712.1567 [hep-ex].
[10] **D0** Collaboration, V. M. Abazov *et al.*, *Phys. Rev. Lett.* **100** (2008) 211802, arXiv:0802.3299 [hep-ex].
[11] **CDF** Collaboration, T. Aaltonen *et al.*, "Measurement of CP Asymmetry in Semileptonic B Decays." CDF Note 9015, 2007.
[12] **D0** Collaboration, V. M. Abazov *et al.*, *Phys. Rev.* **D74** (2006) 092001, arXiv:hep-ex/0609014.
[13] **D0** Collaboration, V. M. Abazov *et al.*, *Phys. Rev. Lett.* **98** (2007) 151801, arXiv:hep-ex/0701007.
[14] **CDF** Collaboration, T. Aaltonen *et al.*, *Phys. Rev. Lett.* **100** (2008) 161802, arXiv:0712.2397 [hep-ex].
[15] **D0** Collaboration, V. M. Abazov *et al.*, arXiv:0802.2255 [hep-ex].

[16] **Heavy Flavor Averaging Group (HFAG)** Collaboration, E. Barberio *et al.*, arXiv:0704.3575 [hep-ex].
[17] **UTfit** Collaboration, M. Bona *et al.*, arXiv:0803.0659 [hep-ph].